ARTICLE

JAAS www.rsc.org/jaas

Interfacial effects during the analysis of multilayer metal coatings by radio-frequency glow discharge optical emission spectroscopy

Part 1. Crater shape and sputtering rate effects

R. Escobar Galindo,* E. Forniés and J. M. Albella

Instituto de Ciencia de Materiales de Madrid (CSIC), E-28049 Cantoblanco, Madrid, Spain. E-mail: rescobar@icmm.csic.es; Fax: +34 91 372 06 23; Tel: +34 91 372 14 20 (ext. 304)

Received 23rd February 2005, Accepted 15th June 2005
First published as an Advance Article on the web 11th July 2005

In depth profile analysis by radio-frequency glow discharge optical emission spectroscopy (rf-GDOES) techniques, the depth resolution mainly depends on the roughening induced during the sputtering and the resulting crater geometry. In this work we have tried to isolate the contributions of the different effects that degrade the depth resolution in GDOES analysis of metal coatings deposited on silicon substrates. First, the existence of an edge well around the crater ("edge effect"), deeper than the crater bottom, results in an initial rise of the quantified profile of the bottom layer before reaching the interface. A second effect is the induced roughening of the crater bottom, which produces a broadening of the interface width. Finally, we have explained the long tails observed after crossing the interface in the metal profiles in terms of the sputtering of material re-deposited at the crater wall. The importance of these effects was tested for the particular case of multilayer stacks consisting of alternating chromium and titanium layers of different thicknesses. Reversing the order of the layers showed the influence of different sputtering rates of the materials in the depth profile. The profiles of materials with high sputtering rate (*i.e.*, chromium in this study) become less affected than material with low sputtering rate (titanium) due to lower mixing of the layers.

Introduction

In the last ten years, the importance of glow discharge optical emission spectroscopy (GDOES) for elemental depth profiling analysis of thin films and coatings has rapidly increased,[1–10] and the number of related scientific publications per year has multiplied by a factor of ten. Nowadays, GDOES competes with more traditional and well-known analytical techniques, such as AES, XPS or SIMS, having a depth resolution comparable to them but without lateral resolution.[11] Using a radiofrequency (rf) source for sputtering extends the application of GDOES to the study of insulator coatings.[1,2,10,12] During GDOES experiments, the samples are sputtered by Ar^+ ions and accelerated neutral species of very low energies (<50 eV). The sputtered atoms are then excited by the plasma and de-excited by photon emission with a characteristic wavelength, enabling element distinction. High sputtering rates, of more than 1 μm min^{-1}, are easily obtained, allowing fast measurements, typically of the order of seconds or a few minutes. Other advantages of GDOES include low matrix effects, no ultra-high vacuum requirements, hydrogen detection and quantification if proper reference materials are used.[12]

Ideally, the crater produced by the sputtering process should have a flat bottom with straight vertical sides that penetrate to the same depth as the bottom. However, in practice this shape is rarely obtained, showing, under certain experimental conditions, a deep well around the edge of the crater.[1] Furthermore, the crater shape changes from one matrix to another, varying during the depth profile of a multilayer coating. As was pointed out by Hoffmann *et al.*,[13] these GDOES-specific effects, namely crater shape, high erosion rate, sample heating or rough vacuum, severely disturb the depth resolution. In particular, the shape of the sputtering crater is crucial as it is very difficult to discriminate the associated edge effects. These edge effects may lead to an increase in the mixing of the consecutive layers in a multilayer system.[14] In fact, good optimisation of the crater shape is an absolute prerequisite for a good depth resolution.[15]

In view of the importance of all these factors in the depth resolution of metallic multilayers, typically used in mechanical, electrical, optical and magnetic applications,[16] we have studied their contribution for the particular case of chromium and titanium alternating multilayers. In this first paper, the crater edge effects have been quantified, measuring the crater shape with the sputtering time for different discharge conditions. The results have been used to minimise the crater shape effects on the depth resolution. Thereafter, other factors, such as roughening of the crater bottom and re-deposition on the crater wall, have been examined in detail. We have observed that the difference in the sputtering rate of these two metals plays an important role in the definition of the interface between them, contributing also to the depth resolution. In addition, the depth where the interface is buried also influences the interface broadening.[17,18] To our knowledge, such effects in multilayer metal systems have not been described previously. In any case, further work on other multilayer systems is still needed in order to extend the representativeness of these results.

In the accompanying paper,[19] all these effects are taken into account in the analysis of different thinner multilayer systems at the nanoscale level. The depth resolution of that system has been evaluated in more detail by the deposition of delta chromium markers (2.5 and 5 nm thick) at different depths in a titanium matrix. These experiments allow the determination of the depth resolution function using deconvolution methods.

Experimental

The deposition of metal layers and multilayers, typically made of alternating titanium and chromium films of different thickness, was performed in a conventional balanced magnetron sputtering system. Table 1 gives a summary of the coatings studied in this work. The deposition of multilayers was made

DOI: 10.1039/b502771c

This journal is © The Royal Society of Chemistry 2005

Table 1 Description of the coating systems studied

Coating	Substrate	Thickness
Cr/Ti/Cr	Silicon	500 nm Cr/500 nm Ti/500 nm Cr 750 nm Cr/2.25 μm Ti/2.5 μm Cr
Ti/Cr/Ti	Silicon	700 nm Ti/700 nm Cr/700 nm Ti
Ti	Silicon	250 nm 1.1 μm 3.4 μm
Cr	Silicon	250 nm 1.0 μm 3.2 μm

using two sputtering sources, placed 6.5 cm away from the substrate holder.

The holder can be rotated to face the sample to each sputtering source and is provided with an automatic position controller in order to control the deposition time for each layer. The deposition rates of the specimens were 125 Å min^{-1} for titanium, and 250 Å min^{-1} for chromium. Other details of the deposition procedure can be found elsewhere.[20] The coatings were deposited onto silicon (100) substrates.

GDOES depth profile analysis of the coatings was completed using a Jobin–Yvon RF GD Profiler[21] equipped with a 4 mm diameter anode and operating at a typical radiofrequency discharge pressure of 650 Pa and a power of 40 W. Table 2 shows the sputtering rates (SR) of the elements used in the study. The discharge settings (power and pressure) were changed during the experiments to investigate the influence of the discharge parameters on the GDOES crater. Quantified profiles were obtained automatically using the standard Jobin–Yvon QUANTUM Intelligent Quantification (IQ) software. The setup was calibrated using standard materials of known composition. The shape and depth of the crater and the coating thickness were measured by profilometry utilizing a Dektak 3030 surface profilometer.

Scanning electron microscopy (SEM) micrographs were obtained with a HITACHI S-2700 using an accelerating potential of 15 kV. Atomic force microscopy observations of the topography of the crater bottom surface were also carried out using a Nascope IIIa model from Digital Instruments.

Results and discussion

Fig. 1 (upper panel) shows a quantified GDOES depth profile of a multilayer coating, consisting of three 500 nm layers, two of chromium and an intermediate layer of titanium, deposited on a silicon (100) substrate. In the lower panel of Fig. 1 a cross-sectional SEM micrograph is presented. The GDOES profile has been overlapped in order to demonstrate the excellent agreement of both techniques to extract the structure of the multilayer system. As can be observed in the GDOES profile, the concentration of chromium is constant along the first layer, the thickness of the layer is well defined and the interface with the titanium layer is very sharp. Nevertheless, as we penetrate deeper in the coating the concentration profiles are less constant and the interfaces become broader (see for instance the tails of the chromium profile at both the Cr/Ti and Ti/Cr

Table 2 GDOES sputtering; rates of the studied elements

Element	Sputtering rate/μm min^{-1}
Chromium	5.3
Titanium	3.5
Silicon (substrate)	3.4

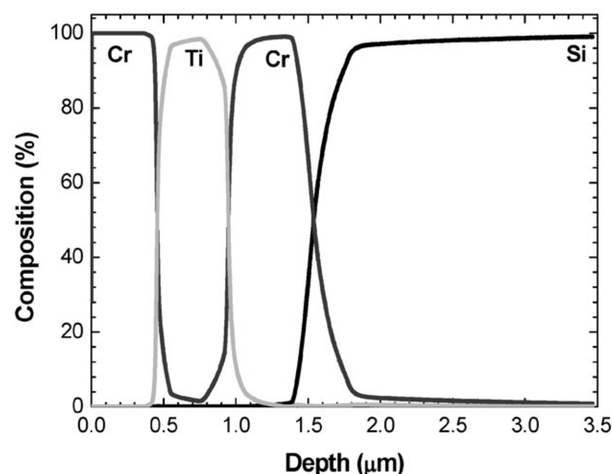

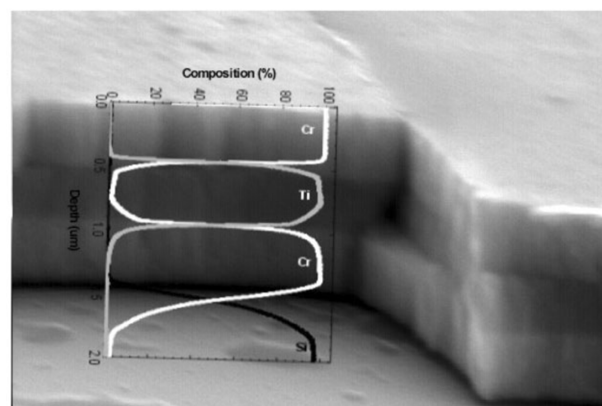

Fig. 1 (Upper panel) Quantified GDOES depth profile of a multilayer Cr/Ti/Cr coating (500 nm thick each layer) deposited on silicon. (Lower panel) Cross-sectional SEM micrograph of the multilayer coating with the GDOES profile overlapped.

interfaces). The interface width (calculated as the measured sputtered depth over which the signal of an element decreases from 84 to 16%[22,23]) in the Cr/Ti interface was measured to be of 50 nm. It increased up to 55 nm and 230 nm at the Ti/Cr and Cr/Si interfaces, respectively.

The loss in resolution of the GDOES profiles with depth has been reported elsewhere[17] and will be the subject of a detailed analysis in nanometric multilayer systems in the accompanying paper.[19] In the present work, we mainly concentrate on the depth resolution loss associated with the non-flat geometry of the crater in thicker films. As will be shown later, under our experimental conditions the well at the edge of the crater penetrates deeper than the central part of the bottom. Therefore, this rim is able to reach the interfaces earlier than the rest of the crater (''crater edge effect''). Also a surface roughening induced by GDOES during the experiment is expected.[24,25] As is discussed below, an additional effect affecting the resolution of the depth profile is the sputtering of material re-deposited on the wall of the crater. In the following sections we describe different experiments performed with the aim of discussing separately each of these effects.

(a) Crater edge effects

In order to quantify the crater shape effect, a single layer of titanium (1.1 μm thickness) was deposited onto a silicon (100) substrate. GDOES discharges were performed on a series of spots in this sample for different sputtering times: (1) 10, (2) 20, (3) 25, (4) 30 and (5) 90 s, corresponding to sputtering depths of 0.5, 1.1, 1.3, 1.6 and 5.2 μm, respectively. Fig. 2(a) shows the quantified depth profile after the longest GDOES experiment of 90 s. The sputtered depths corresponding to the different

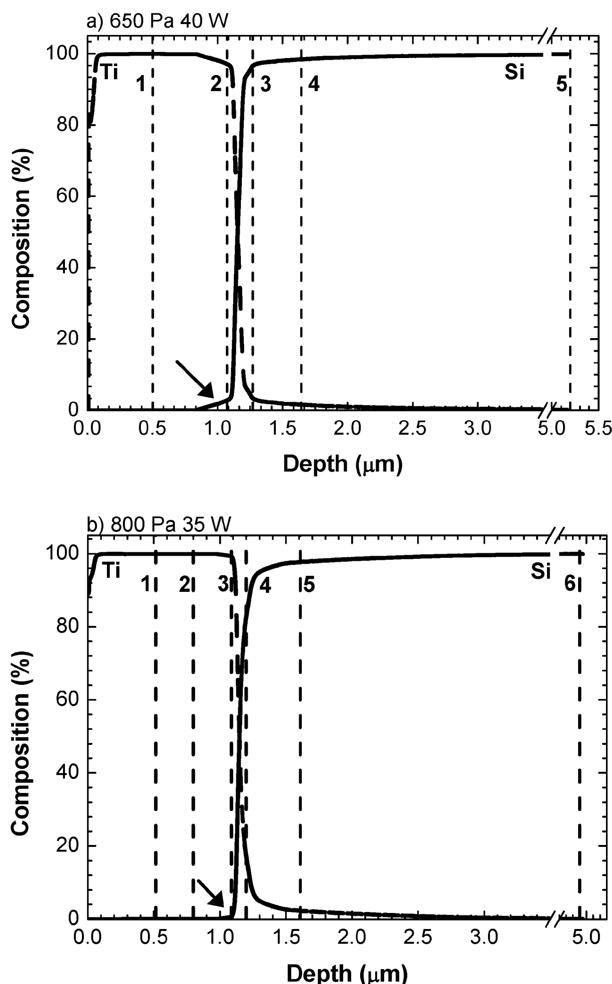

Fig. 2 Quantified GDOES depth profiles of a single layer of 1.1 μm titanium deposited on silicon. The experimental conditions were (a) 650 Pa and 40 W, and (b) 800 Pa and 35 W. The broken vertical lines indicate the sputtered depth corresponding to different GDOES experiments. The arrows indicate the initial upraise of the silicon signal due to the crater edge effect.

discharge experiments are marked with numbered vertical dashed lines (1–5).

Until a sputtered depth of approximately 800 nm (marked by vertical broken line (1)), the titanium profile is kept constant at 100% content. Afterwards (sputtered depth (2)), there is a smooth decrease in the titanium content with depth corresponding to the initial detection of silicon (see arrow in Fig. 2(a)). This behaviour, similar to that observed at the different interfaces in Fig. 1, remains until the titanium–silicon interface is properly detected at 1.1 μm by a very sharp increase of the substrate profile (3). However, the titanium signal does not disappear immediately (4) and only when a depth of several microns is reached, is the 100% silicon content found (5).

Fig. 3 shows the crater shape of the GDOES experiment performed for 20 s. This experiment corresponds to the vertical broken line number 2 in Fig. 2(a). As can be observed, the edge of the crater (approximately 1% of the total volume) reaches the silicon substrate up to a depth of 1.3 μm while the rest of the sputtered crater remains inside the titanium layer at a depth of 1.0 μm. This difference in height (*d* in Fig. 3) represents a difference of 30% in the sputtering rate. The presence of a crater shoulder, right after the edge, also alters the flatness of the central part of the crater and also affects the depth resolution, as discussed below. In addition, the sputtered material, accumulated on the periphery, produces a higher crater wall.

Fig. 4(a) presents the evolution of the crater shape with the sputtering time. The different crater profiles correspond to the

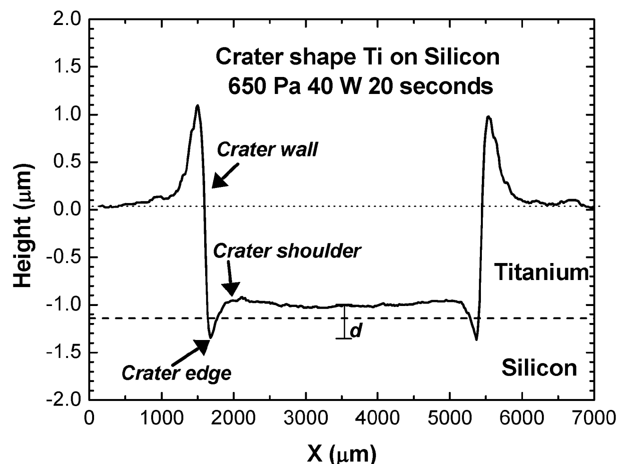

Fig. 3 Crater shape after a GDOES experiment performed for 20 s on a single layer of 1.1 μm titanium deposited on silicon. This crater corresponds to the vertical broken line number 2 in Fig. 2(a). The height *d* represents the difference between the depth of the crater edge and the centre of the crater bottom.

sputtering depths numbered 1–5 in Fig. 2(a). After 10 s (crater 1), the bottom of the crater remains inside the metal layer, resulting in the 100% content of titanium shown in the depth profile of Fig. 2(a). As was mentioned above, after 20 s (crater 2) the well at the edge of the crater reaches the silicon substrate, producing an initial rise of the silicon content in Fig. 2(a). If we increase the sputtering time to 25 s (crater 3), both the edge and the centre of the crater are inside the silicon substrate. However, a small amount of titanium (approximately 3%) is still present in the depth profile of Fig. 2(a). This Ti contribution may be due to the shoulder that follows the crater edge observed in crater profile 3 of Fig. 4(a). This shoulder is still eroding the titanium layer, while the edge and the centre of the crater already reach the substrate. After 30 s of sputtering (crater 4), there is still approximately 1.6% of titanium detected in the depth profile of Fig. 2(a). Nevertheless, we can see in Fig. 4(a) that the whole crater 4 (shoulder included) is well inside the silicon substrate; so no titanium signal should be expected. A plausible explanation could be the sputtering of titanium atoms previously re-deposited on the wall of the substrate. It should be noticed that the material accumulated on top of the outer crater edge increases with sputtering time. Finally, after 90 s of sputtering (crater 5), the titanium signal

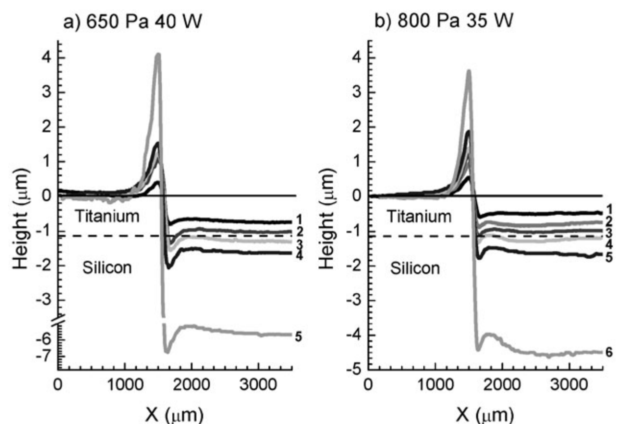

Fig. 4 Evolution of the crater shape with the GDOES sputtering time for a single layer of 1.1 μm titanium deposited on silicon. In (a) the experimental conditions were 650 Pa and 40 W, with the numbers beside each profile corresponding to the sputtering times of Fig. 2(a): (1) 10, (2) 20, (3) 25, (4) 30 and (5) 90 s. In (b) the experimental conditions were 800 Pa and 35 W and the numbers correspond to the sputtering times of Fig. 2(b): (1) 12, (2) 22, (3) 24, (4) 29, (5) 35 and (6) 90 s.

has already vanished and only the silicon signal is detected. Note that, apart from the edge and shoulder already discussed, all the crater profiles of Fig. 4(a) are very flat (between 25 and 30 nm).

(b) Optimisation of the crater shape

It is well known that by changing the discharge parameters, namely pressure and power, the geometry of the GDOES crater can be modified.[26] The aim of these changes is improving the crater flatness, avoiding either concave or convex geometries of the bottom. In our study, we have varied the pressure and power of the rf-GDOES discharge to minimise the crater edge height *d*, as defined in Fig. 3. To this end, GDOES experiments were performed on a silicon wafer (100) oriented, varying the discharge pressure in a range from 450 to 850 Pa and the power from 30 to 50 W until reaching a sputtered depth of 7 μm. Fig. 5 summarises the results where the diameter of the circles scales to the crater edge depth, *d*. As an example, the depth of the edge measured at 40 W and 650 Pa was of 1.2 μm (dark circle in Fig. 5). As can be appreciated, there is a clear trend on the crater edge depth, increasing with the discharge power for powers higher than 35 W. The crater edge depth also increases while decreasing the pressure, as long as we perform the experiment at pressures below 800 Pa. The minimum crater edge depth was obtained at those limits (35 W and 800 Pa) and was found to be 250 nm (circle marked with an arrow in Fig. 5).

In order to estimate the effect of the crater edge on the depth profiles, we performed GDOES analysis on a 1.1 μm titanium layer on silicon at 800 Pa and 35 W (minimum crater edge depth). GDOES discharges were performed during six different times on different areas of the sample: (1) 12, (2) 22, (3) 24, (4) 29, (5) 35 and (6) 90 s, corresponding to sputtering depths of 0.5, 0.8, 1.0, 1.2, 1.6 and 4.9 μm, respectively. In Fig. 2(b) the quantified depth profile is shown after the longest GDOES experiments of 90 s. As in Fig. 2(a), the sputtered depths corresponding to the different discharge experiments are marked in Fig. 2(b) with numbered vertical dashed lines (1–6). In Fig. 4(b) the evolution of the crater shape at these new discharge conditions is followed with the sputtering time. The different crater profiles correspond to the sputtering depths numbered (1–6) in Fig. 2(b).

The first clear observation is that, up to the interface (sputtered depths marked with lines 1–3), the titanium depth profile in Fig. 2(b) is more squared than the corresponding one in Fig. 2(a). There is a constant 100% content of titanium in the whole coating, with no sign of the silicon substrate (see arrow in Fig. 2(b)) until an abrupt change in the composition is detected at the interface. This result confirms the proposed hypothesis suggesting the change in the slope of the titanium profile is due to the crater edge eroding the substrate. As can be observed in Fig. 4(b) crater 3, the depth *d* of the well at the edge is approximately of 100 nm. Such a small depth does not result in a significant detection of the silicon substrate before reaching the interface.

On the other hand, it can be observed that, after crossing the interface, the titanium contribution that remains is higher than in Fig. 2(a). At 1.2 μm (sputtered depth 4) there is still 18% of titanium detected by GDOES, while for the experiments performed at 650 Pa and 40 W the remaining titanium at the same depth was only 3%. This seems to confirm the role of the shoulder in the depth profiles, as explained above. In Fig. 4(b), the shoulder following the edge of crater 4 is clearly still eroding the titanium layer. But the contribution of the shoulder, even higher than in Fig. 4(a), is not enough to justify such a high titanium signal. As can be observed, the central part of crater 4 is not as flat as in Fig. 4(a), so it seems plausible to conclude that it also contributes to increasing the content of titanium detected during the sputtering process. As in the previous case, the re-deposition of titanium on the crater walls is the reason for detecting approximately 2% of titanium at 1.6 μm (sputtered depth 5), when the crater is well below the interface (see Fig. 4(b)). This will be discussed in the following section (d). Deeper in the substrate (sputtered depth 6) there is only a silicon signal.

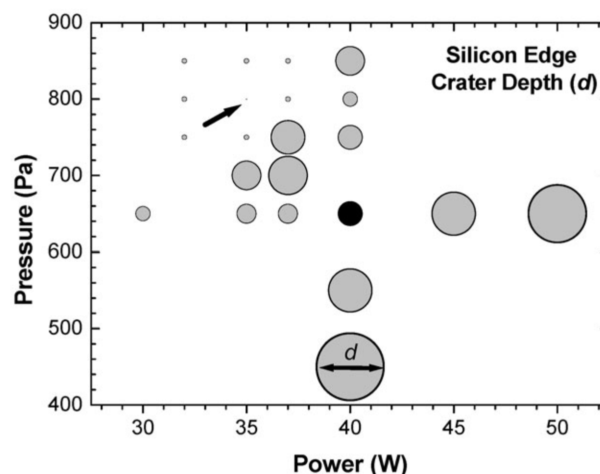

Fig. 5 GDOES discharge pressure *versus* power map for silicon (100) sputtered at 7 μm. The size of the circles scales to the crater edge depth, *d*. The black circle indicates the experiments at 650 Pa and 40 W. The arrow points out the conditions where the minimum *d* was found (800 Pa and 35 W).

The magnitude of the crater edge effect is clearly dependent on the sputtering depth, as can be demonstrated in the GDOES profiles of Fig. 6(a) for three titanium layers with thicknesses of 0.25, 1.1 and 3.4 μm deposited on silicon. The profiles were performed at 650 Pa and 40 W. We can clearly observe in Fig. 6 how the area *A* below the silicon curve (ascribed to the crater edge effect), before the interface, increases in a linear way with the coating thickness by a factor 2.87 with a standard deviation of 0.07 (2.87 ± 0.07). Also, the contribution of titanium detected after the interface (area *B* in Fig. 6(a)) increases linearly with depth by a factor 3.08 ± 0.11. The increase of the area *B* is attributed both to the growth of the crater shoulder and the sputtering of material re-deposited on the crater walls (see section (c)). Together with these effects associated with the titanium tails, there is an interface broadening due to the roughening of the crater bottom (see section (d)). This produces of loss of resolution with depth. The interface widths of Fig. 6(a) were measured, observing a linear increase from a value of 20 nm for the 250 nm coating up to 70 and 250 nm for the 1.1 and 3.4 μm coatings, respectively.

Summarizing this section, we can state that the crater edge and shoulder associated with the sputtered areas in GDOES discharges strongly influence the depth profile resolution at the interface. The edge starts eroding the substrate earlier than the central part of the crater, causing an increase of the signal of the substrate in the vicinity of the interface. This increase depends linearly on the thickness of the coating. By optimising the experimental conditions to minimize the edge height, it is possible to improve the interface resolution but at the expenses of a loss in the flatness of the crater and increasing the redeposition from the crater walls. This loss of flatness may worsen the depth profiles of multilayer coatings.

(c) Re-deposition on the crater wall

As was indicated above (sections (a) and (b)) the profiles analysed in Figs. 1 and 2 show that, once the crater bottom reaches the Si surface, there is a long tail in the profile of the adjacent metal (Ti or Cr in either case). In fact, the same behaviour is observed at the interfaces between the individual

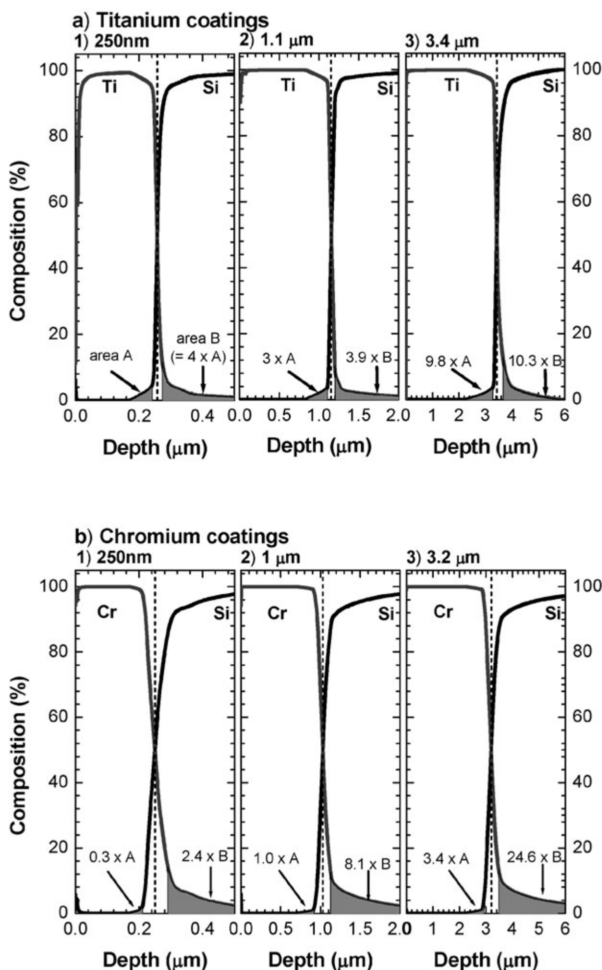

Fig. 6 Comparison of GDOES depth profiles of (a) titanium and (b) chromium single layers with different thicknesses. The areas under the initial silicon upraise and the metal tails, respectively, before and after the interface, are indicated. These areas are normalised to the values of the 250 nm titanium coating areas (*A* and *B*). Note the depth scale differences of the graphs. The experiments were performed at 40 W and 650 Pa.

metal layers of Fig. 1, though masked by the effects described in the previous sections. In the case of metal/Si interfaces, we attributed these long tails to the sputtering of the metal atoms re-deposited on the crater walls. Actually, the crater shapes of Figs. 3 and 4 indicate that large amounts of the sputtered material are accumulated on the crater rim. Therefore, it is expected that the last metal, sputtered before the silicon, is still contaminating the whole crater walls, thus appearing long after the crater bottom has surpassed the metal/Si interface. This effect should be also modulated by the sputtering rate of the metal, resulting in larger tails for those metals with higher sputtering rates (*i.e.*, chromium compared with titanium), in agreement with the observed profiles for Ti and Cr in Fig. 1.

In order to confirm this working hypothesis, we have deposited three chromium layers with thicknesses of 0.25, 1.0 and 3.2 μm on silicon. The profiles, performed at 650 Pa and 40 W, are shown in Fig. 6(b). The first observation is the very small area under the silicon curve before the interface, ascribed in the previous section to the crater edge effect. This area is approximately three times smaller than the area observed in the different titanium coatings in Fig. 6(a) with the same thickness. In fact, to obtain a similar edge effect in chromium coatings compared with titanium layers, approximately four times thicker coatings must be deposited. For example, 250 nm titanium and 1 μm chromium layers have the same area *A*. Although smaller, the area also increases linearly with depth, as in the case with the titanium coatings but with a higher factor of 3.65 ± 0.07. This behaviour can be explained as the crater shapes developed on the Cr layers are similar to the ones shown in Fig. 4(b) for the experiments performed on the titanium layer at 800 Pa and 35 W. Thus, the difference between the depth of the edge well and the centre of the crater is much smaller than for the titanium layers but the shoulders are larger and the crater less flat. On the other hand, as we hypothesized, the metal contribution after the interface is considerably larger (approximately 2.4 times) for the chromium layers than for the titanium at the same coating thickness. This contribution, related to the sputtering of material re-deposited on the crater wall, increases linearly with the thickness of the coatings with a factor 3.18 ± 0.04.

As was mentioned above, despite the different experimental conditions applied to the analysis of the 1 μm Cr/Si in Fig. 6(b)2 (GDOES performed at 650 Pa and 40 W) and the 1.1 μm Ti/Si of Fig. 2(b) (800 Pa and 30 W), the crater shapes resulting from both experiments are very similar. Nevertheless, some important differences can be observed. The areas before and after the interface are 1.48 and 1.3 times larger for the Cr/Si system, respectively. These values are in the same order of magnitude as the ratio between the sputtering rates of chromium and titanium ($SR_{Cr}/SR_{Ti} = 1.5$). Therefore, it is not only the shape of the crater but also the sputtering rate of the material which determines the crater edge and re-deposition effects observed in the GDOES depth profiles.

The Cr/Si interfaces are also wider than the Ti/Si ones, increasing linearly from 60 nm for the 250 nm coating up to 140 and 410 nm for the 1.0 and 3.2 μm coatings, respectively. In the following section a more detailed study of the interface broadening is given.

(d) Roughening of the crater bottom

In the previous sections we have shown that changing the experimental conditions or the metal coating to reduce the crater edge depth results in a loss of the flatness of the crater bottom. This loss produces a broadening of the coating/substrate interface. Together with the crater edge and re-deposition effects, it has been reported in the literature that GDOES experiments induce surface roughening[24,25] in the nanometre scale on initially rough surfaces.

In Fig. 7 two AFM graphs showing the surface of a 3.4 μm titanium coating on silicon (see Fig. 6(a)3) are presented. On the left, we can observe the surface of the as-deposited sample. The surface has a root-mean-square (RMS) roughness of 19 nm. On the right is the surface of the centre of the crater after a GDOES experiment of 7 s at 650 Pa and 40 W.

This time corresponds to a sputtering depth of approximately 300 nm. The appearance of small holes on the surface of the coating can clearly be observed. These holes have a typical diameter of 800 nm and a depth of 70 nm. The RMS roughness of the surface increases up to 28.5 nm.

That the roughening of the surface increases with the sputtering time is well documented in the literature and, obviously, it contributes to the mixing of the coating and the substrate at the interface between them, thus broadening the interface width.[24,25] As a consequence of this mechanism, the concentration profiles become less abrupt at the interface, leading to a loss of resolution. Moreover, the widening of the interface should be larger for deeper interfaces, *i.e.*, when thicker layers are deposited on top of a flat substrate (polished Si wafers in this work). In a multilayer system this effect produces broader interfaces as one penetrates across successive multilayers. A further analysis of the problem following the roughness of the samples at different sputtering times using AFM experiments is under progress.[27]

A novel aspect of this work lies in the fact that the layer mixing at the interface is modulated by the sputtering rates of the adjacent materials. Metal coatings with higher sputtering

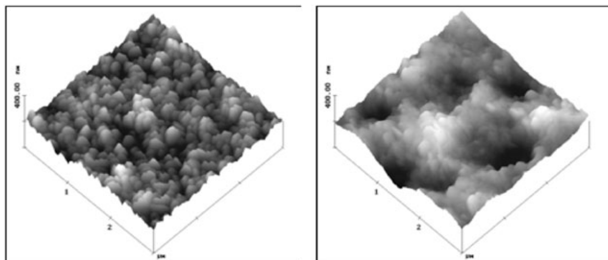

Fig. 7 AFM graphs showing the surface topography of a 3.4 μm titanium coating on silicon, (left) as deposited and (right) after a GDOES experiment for 7 s at 650 Pa and 40 W.

rates (*i.e.*, Cr, in the multilayer system of Fig. 1) are supposed to contribute with a larger concentration at the interface than metals with lower sputtering rate (*i.e.*, Ti). In other words, Ti profiles should be sharper than Cr profiles, under the same experimental conditions, as has been observed in the profiles shown in Fig. 1. This is clearly demonstrated for the deposited metal monolayers of Fig. 6(a) and 6(b). For a similar coating thickness the Cr/Si interface was always wider than the Ti/Si interface. As an example, the interface width at 3.2 μm depth of the Cr/Si coating was 410 nm, while that of the Ti/Si at 3.4 μm was only 250 nm.

To prove this assertion in multilayer systems, we have deposited a similar but reversed stacking system to that of Fig. 1, made of three 700 nm thick layers, Ti/Cr/Ti, on top of a silicon substrate. The GDOES concentration profiles are depicted in Fig. 8.

As can be clearly observed, the Ti profile before the Ti/Cr interface is less abrupt than the corresponding first Cr profile of Fig. 1. The crater edge effect described in the previous sections (*i.e.*, the initial rise of the Cr signal) is enhanced at the Ti/Cr interface by the difference in SR between Ti and Cr. This is because the crater edges reaching the Cr erode more material, and thus the Cr signal is increased dramatically. The same effect is observed in the Ti/Cr interface of Fig. 1. This behaviour can be compared with the Cr/Ti and Ti/Si interfaces of Fig. 8 when the crater edge effect is very much reduced even at higher depths.

Despite this crater edge effect the width of the Ti/Cr interface in Fig. 8 is 60 nm, that is, only 10 nm higher than the Cr/Ti interface of Fig. 1, but 200 nm deeper. On the other hand the Cr/Ti interface of Fig. 8 is 203 nm, much wider than the 55 nm measured for the Ti/Cr interface of Fig. 1. Finally, the Ti/Si interface is much narrower that the Cr/Si one. Although located 2.1 μm deeper, the Ti/Si interface was measured to be of 150 nm instead of the 250 nm obtained for the Cr/Si

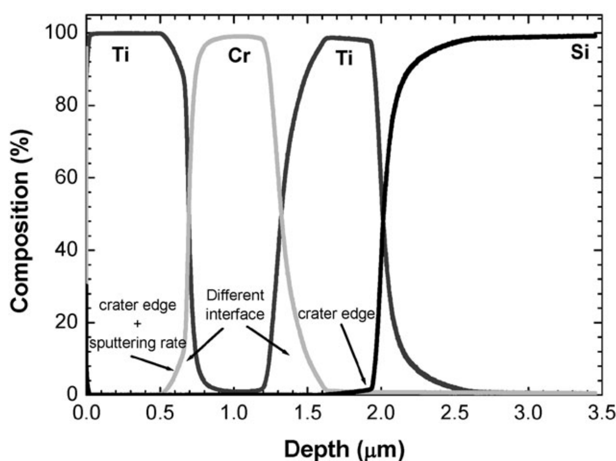

Fig. 8 Quantified GDOES depth profile of a multilayer Ti/Cr/Ti coating (700 nm thick each layer) deposited on silicon.

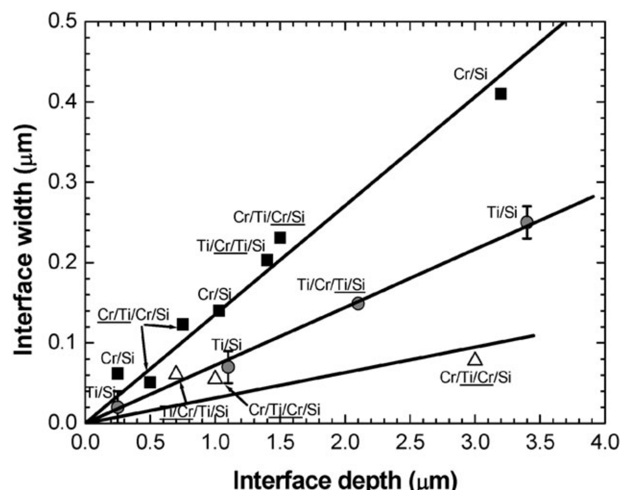

Fig. 9 Relationship between the width and depth of the different interfaces studied in this work. The three solid lines represent linear fits of the data grouped according to the different types of interfaces: Cr/Ti or Cr/Si (closed squares), Ti/Si (grey circles) and Ti/Cr (open triangles).

interface at 1.5 μm. As a conclusion, for similar depths, the interfaces separating elements with higher and lower sputtering rates are much wider when the high sputtering element is sputtered first. The influence of the interface depth on the depth resolution is shown in Fig. 9, where all the different interface widths of the different coating systems studied (from Figs. 1, 6(a), 6(b), and 8) are plotted *versus* the interface depth.

It is noticeable that all interface widths increase linearly with depth. The same observation was reported by Shimizu *et al.* for the case of atomically flat alumina/aluminium interfaces[17] and by Beck *et al.*[18] for Ti/Al multilayers. In this last work a comparison is made between the interface width increase observed during GDOES and AES experiments. However, in our work, we have observed that this increase is determined by the elements present at the interfaces (see Table 3). The interface widening is more pronounced with depth when the material before the interface has a higher sputtering rate (*i.e.*, Cr) than the material after it (*i.e.*, Ti or Si). The reason why all the Cr/Ti and Cr/Si interfaces (closed squares in Fig. 9) lie together on the same linear fit is the practically identical SR of both Ti and Si (see Table 2). This fact stresses the strong relationship between the SR of the material and the interface width. The width of these interfaces increases 154 ± 46 nm for each micron by which the interface is buried. On the other hand, crossing the interface from a material with a lower SR (*i.e.*, Ti) to a material with a higher one (*i.e.*, Cr), the widening of the interface increases much less with the interface depth. For example a Ti/Cr interface located at 3 μm has a much smaller width (78 nm) than a Cr/Si at 3.2 μm (410 nm). The fit of the Ti/Cr interface widths is worse than that of Cr/Ti but nevertheless gives a lower value of 56 ± 30 nm per μm. Finally, the fit of the Ti/Si interface (both elements with almost equal SR) widths results in an intermediate value of 72 ± 7 nm per μm. Shimizu *et. al.*[26] reported that, for atomically flat interfaces, the degradation of depth resolution is due to variations of 6% in the sputtering rate across the crater. In our work we are looking at SR differences across the interfaces. The differences we obtained were up to 35%, confirming the great importance of the SR in the proper determination of the depth resolution in GDOES experiments.

It is important to note that the tendency of the width of the interfaces in Fig. 9 is similar for all the interfaces of each studied type (high SR → low SR, same SR or low SR → high SR). The width only depends on the interface depth, regardless of whether the interfaces belong to a mono- or a multilayer coating. This implies that, in multilayer stacks, previously

Table 3 Relation between the interface width and the depth where the interface is located for different types of interfaces. The calculated values are the slopes of the linear fits of Fig. 9

Interface elements	Interface width per depth/nm per μm	Type of interface
Chromium/Titanium Chromium/Silicon	154 ± 46	High SR → Low SR
Titanium/Silicon	72 ± 7	Same SR
Titanium/Chromium	56 ± 30	Low SR → High SR

sputtered layers do not influence the following interface resolutions at least for coatings in the thickness range studied here (above 250 nm). A possible explanation could be as follows. It is obvious that after each interface there is a continuous change in the crater shape.[14] For example, in the Ti/Cr/Ti system of Fig. 8, before the first interface there is a crater-edge dominant shape (similar to the ones of Fig. 4(a)). After crossing the interface this shape tends to one more similar to those of Fig. 4(b) (less flat, fewer edges, more shoulders). If the layers are thick enough, the change in shape is complete and, therefore, when the crater reaches the next Cr/Ti interface it has the same shape as a Cr monolayer. Thus, for such thick multilayers, GDOES interface profiles retain no memory of the previous sputtered layers.

(e) Final remarks: overall influence of the layer thickness on the depth resolution

In order to emphasise the influence of the coating thickness on the depth resolution, we deposited a Cr/Ti/Cr multilayer coating, consisting on two chromium layers of 750 nm and 2.5 μm, with a titanium layer of 2.25 μm in between. The GDOES depth profile of this system shown in Fig. 10 is practically a scale up of the one in Fig. 1. Note that the shape of the Cr, Ti and Si profiles are practically the same, though all the effects discussed in the previous sections are magnified in Fig. 10.

Therefore, the crater edge effect is obviously much more severe (approximately 6 times larger) before the Ti/Cr interface of Fig. 10 (A′) than the one in Fig. 1. The enlargement of the crater edge effect for the Cr/Ti (A) and Cr/Si (A″) interfaces is less evident due to the shape of the crater inside the chromium layer, as explained above. Furthermore, the different interfaces of Fig. 10 (B, B′ and B″) are wider than the ones of Fig. 1. This increase of the interface width with the coating layer thickness

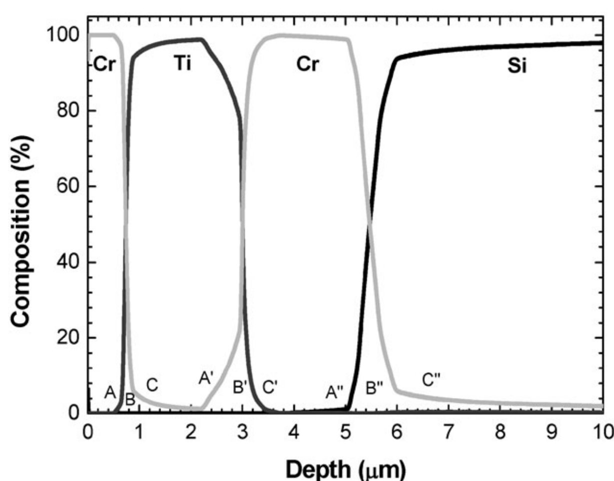

Fig. 10 Quantified GDOES depth profile of a 750 nm Cr/2.25 μm Ti/2.5 μm Cr multilayer coating deposited on silicon. Letters indicate the effects discussed in the paper which are summarised for the different interfaces: crater edge effect (A, A′, A″), interface widening (B, B′, B″) and sputtering of re-deposited material (C, C′, C″).

is in agreement with the analysis of Fig. 9. Finally, the sputtering of re-deposited material in the crater walls is evidently higher for chromium in Fig. 10 (C and C″) than in Fig. 1 (2 and 4 times, respectively). This result is in conformity with the observations shown before in Fig. 6(b) for the chromium monolayers.

Conclusions

From the above results it follows that three different effects, related to layer mixing during sputtering, contribute to a greater or lesser extent to the interface broadening in multilayer systems, thus affecting the depth resolution in GDOES experiments. All these effects arise from the particular shape of the sputtering crater and can be can be summarised as follows.

(a) **Edge effects**, especially those associated to the deep well at the crater rim, which degrade the depth resolution of the profile before the interface. They contribute to a broadening of the profiles, producing an initial rise of the quantified profile of the subsequent layer before reaching the interface (or a less steep decrease of the profile of the top metal). This contribution was found to be more apparent in the interfaces where the first metal (*e.g.*, Ti) has a lower sputtering rate than the second metal (*e.g.*, Cr), and is more visible for deeper interfaces. The extent of the rise area gives a measure of the depth of the edge well. In the case of Ti, the edge effects are diminished by reducing the power and increasing the pressure of the discharge, but at the expense of a loss in the flatness of the crater.

(b) **Re-deposition and sputtering from the crater wall**. During the glow discharge process, some layer material sputtered from the bottom is thought to be re-deposited onto the crater wall, where it is sputtered again. As the depth of the crater increases, the deposition on the wall should be higher and also the contamination or mixing with the material being analysed. The effect is supposed to cause the observed long tail of the profile curve after passing the interface. The tail is more apparent in deep interfaces, and for the case when the first metal or the deposited layer (*e.g.*, Cr) has a higher sputtering rate than the second metal or substrate (*e.g.*, Ti or Si).

(c) **Roughening of the crater bottom**, due to the continuous sputtering of the analysed layer. It increases with the sputtering time (or depth) and produces a broadening of the step profiles of metal multilayers at the interface. The broadening is wider in interfaces where the top metal (*e.g.*, Cr) has a higher sputtering rate than the underneath metal or substrate (*e.g.*, Ti or Si). For a given interface, its width increases linearly with depth regardless of the detailed structure of the whole system (monolithic or multilayered).

Acknowledgements

The authors wish to thank P. Chapon (Jobin–Yvon) and N. Bordel (Universidad de Oviedo) for their valuable comments during the preparation of the manuscript. The authors are also indebted to L. Vázquez and M. A. Auger (ICMM) for the AFM measurements and help with the sputtering deposition of the multi-layer coatings, respectively.

References

1 *Glow Discharge Optical Emission Spectrometry*, eds. R. Payling, D. Jones and A. Bengtson, John Wiley & Sons, 1997.
2 M. R. Winchester and R. Payling, *Spectrochim. Acta, Part B*, 2004, **59**, 607.
3 W. B. Teo and K. Hirokawa, *Surf. Interface Anal.*, 1988, **11**, 533.
4 W. B. Teo and K. Hirokawa, *Surf. Interface Anal.*, 1989, **14**, 143.
5 Z. Weiss, *Czech. J. Phys.*, 1990, **40**, 237.
6 Z. Weiss, *Surf. Interface Anal.*, 1990, **15**, 791.
7 Z. Weiss, *Surf. Interface Anal.*, 1990, **15**, 775.
8 Z. Weiss, *Surf. Interface Anal.*, 1991, **17**, 641.
9 Z. Weiss, *Spectrochim. Acta*, 1992, **47B**, 859.

10 F. Präßler, V. Hoffmann, J. Schumann and K. Wetzig, *J. Anal. At. Spectrom.*, 1995, **10**, 677.
11 S. Oswald and S. Baunack, *Thin Solid Films*, 2003, **425**, 9.
12 V. Hodoroaba, W. E. S. Unger, H. Jenett, V. Hoffmann, B. Hagenhoff, S. Kayser and K. Wetzig, *Appl. Surf. Sci.*, 2001, **179**, 30.
13 V. Hoffmann, R. Dorka, L. Wilken, V. D. Hodoroaba and K. Wetzig, *Surf. Interface Anal.*, 2003, **35**, 575.
14 A. Quentmeier, in *Glow Discharge Optical Emission Spectroscopy*, eds. R. Payling, D. G. Jones and A. Bengston, John Wiley & Sons, New York, 1997, Section 7.1 and Section 7.2.
15 J. Angeli, A. Bengston, A. Bogaerts, V. Hoffmann, V. Hodoroaba and E. Steers, *J. Anal. At. Spectrom.*, 2003, **18**, 670.
16 A. Leyland and A. Matthews, *Surf. Coat. Technol.*, 2004, **177–178**, 317.
17 K. Shimizu, H. Habazaki, P. Skeldon, G. E. Thompson and R. K. Marcus, *Surf. Interface Anal.*, 2001, **31**, 869.
18 U. Beck, G. Reiners, Th. Wirth, V. Hoffmann and F. Präβler, *Thin Solid Films*, 1996, **290–291**, 57.
19 R. Escobar Galindo, E. Forniés and J. M. Albella, *J. Anal. At. Spectrom.*, 2005, DOI: 10.1039/b502774h.
20 M. A. Auger, R. Gago, M. Fernández, O. Sánchez and J. M. Albella, *Surf. Coat. Technol.*, 2002, **157**, 26.
21 http://www.jobinyvon.com.
22 S. Hofmann in *Practical Surface Analysis by Auger and X-ray Photoelectron Spectroscopy*, eds. D. Briggs and M. P. Seah, John Wiley & Sons, New York, 1983, ch. 4.
23 S. Hofmann, *Surf. Interface Anal.*, 1999, **27**, 825.
24 K. Shimizu, H. Habazaki, P. Skeldon, G. E. Thompson and G. C. Wood, *Surf. Interface Anal.*, 1999, **27**, 950.
25 K. Shimizu, G. M. Brown, H. Habazaki, K. Kobayashi, P. Skeldon, G. E. Thompson and G. C. Wood, *Surf. Interface Anal.*, 1999, **27**, 153.
26 K. Shimizu, H. Habazaki, P. Skeldon, G. E. Thompson and G. C. Wood, *Surf. Interface Anal.*, 2000, **29**, 155.
27 R. Escobar Galindo, L. Vazquez and J. M. Albella, 2004, to be published.